

# Global and local contributions to curvature of a moderately keratoconic cornea

WF Harris and WDH Gillan

Department of Optometry, Auckland Park Campus, University of Johannesburg, PO Box 524, Auckland Park, 2006 South Africa

Received 12 March 2008; revised version accepted 31 March 2008

## Abstract

A recent paper describes a simple model for determining global and local contributions to corneal curvature. The model makes use of measurements of the curvature of the anterior and posterior surfaces of the cornea. The purpose of this paper is to illustrate application of the model. The model is applied to a moderately keratoconic cornea. The curvature of the posterior surface of the cornea exhibits greater variation than that of the anterior surface. Global effects dominate. The variation of the ortho-antispherical component of global curvature suggests an important role for the lids in keratometric variation.

## Introduction

A recent paper<sup>1</sup> examines the power of the anterior and posterior surfaces of a moderately keratoconic cornea. The back surface exhibits considerably less variation than the front surface. This is to be expected because of the much greater difference in index of refraction across the front surface than across the back surface. While power is appropriate for studies of optical effects, curvature is the more appropriate property when one is interested in the underlying causes of variation in corneal power. Accordingly the purpose of this paper is to re-examine the same cornea but in terms of surface curvature instead of power. We also make use of the theory developed in a second recent paper<sup>2</sup> to estimate the global and local contributions to curvature with a view to gaining insight into the possible causes of the variation in curvature of the cornea.

## The surface curvatures

Table 1 gives the raw data upon which this study was based. It lists the first five of 25 sets of readings of radius  $r$  of curvature along principal meridians of

the anterior and posterior surfaces of the cornea.  $r_1$  is the radius of curvature along a principal meridian at angle  $A_1$  and  $r_2$  the radius of curvature along the principal meridian at  $A_1 + 90^\circ$ . The thickness  $t$  is also listed. For more details the reader is referred to the earlier paper<sup>1</sup>.

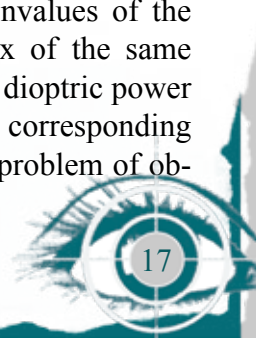
**Table 1** The first five of 25 measurements of radius of curvature along the principal meridians ( $r_1$  along  $A_1$  and  $r_2$  along  $A_1 + 90^\circ$ ) of the anterior and posterior surfaces of the cornea. The last row gives the radii and principal meridians for the mean given in Table 3. The thickness is also given.

Anterior surface			Thick- ness	Posterior surface		
$r_1$ /mm	$A_1$ /degrees	$r_2$ /mm		$r_1$ /mm	$A_1$ /degrees	$r_2$ /mm
7.78	146	7.26	413	6.73	153	5.77
7.78	146	7.32	418	6.72	152	5.86
7.81	140	7.27	415	6.90	145	5.87
7.82	140	7.29	418	6.84	152	5.85
7.85	142	7.30	419	6.97	151	5.87
⋮	⋮	⋮	⋮	⋮	⋮	⋮
7.82	143	7.29	415	6.81	151	5.83

The curvature  $\kappa$  along a meridian is calculated by means of

$$\kappa = \frac{1}{r}$$

The results for the first five sets of measurements are given in Table 2.  $\kappa_1$  and  $\kappa_2$  are the curvatures along the principal meridians at angles  $A_1$  and  $A_1 + 90^\circ$  respectively.  $\kappa_1$  and  $\kappa_2$  are the eigenvalues of the surface curvature matrix  $\kappa$ , a matrix of the same mathematical nature as the symmetric dioptric power matrix  $F^2$ .  $A_1$  and  $A_1 + 90^\circ$  define the corresponding eigenspaces. The reverse eigenvalue problem of obtaining  $\kappa$  from  $\kappa_1$ ,  $\kappa_2$  and  $A_1$  is



exactly the same as obtaining **F** from its principal powers and principal meridians.<sup>2</sup> The coefficients  $\kappa_I$ ,  $\kappa_J$  and  $\kappa_K$  of surface curvature are obtained from  $\kappa$ ;  $\kappa_I$  is the spherical coefficient,  $\kappa_J$  the ortho-antispherical coefficient and  $\kappa_K$  the oblique anti-spherical coefficient.<sup>2</sup> They are listed in Table 3.

**Table 2** Principal meridional curvatures and mean (last row) for the first and second surfaces of the cornea

Anterior surface			Posterior surface		
$\kappa_I$ /mm	$A_I$ /degrees	$\kappa_2$ /mm	$\kappa_I$ /mm	$A_I$ /degrees	$\kappa_2$ /mm
128.5	146	137.7	148.6	153	173.3
128.5	146	136.6	148.8	152	170.6
128.0	140	137.6	144.9	145	170.4
127.9	140	137.2	146.2	152	170.9
127.4	142	137.0	143.5	151	170.4
⋮	⋮	⋮	⋮	⋮	⋮
127.9	143	137.2	146.8	151	171.5

**Table 3** The spherical  $\kappa_I$ , ortho-antispherical  $\kappa_J$  and oblique antispherical  $\kappa_K$  coefficients of surface curvature, the mean coefficients  $\bar{\kappa}_I$ ,  $\bar{\kappa}_J$  and  $\bar{\kappa}_K$ , the mean surface curvature matrix  $\bar{\kappa}$  and the variance-covariance matrix **S** of the coordinate vector  $(\kappa_I \ \kappa_J \ \kappa_K)^T$  for the anterior and posterior surfaces of the cornea. Only the upper-triangular entries are given explicitly in symmetric matrices.

	Anterior surface			Posterior surface		
	$\kappa_I/D$	$\kappa_J/D$	$\kappa_K/D$	$\kappa_I/D$	$\kappa_J/D$	$\kappa_K/D$
	133.1	-1.7	4.3	160.9	-7.3	10.0
	132.6	-1.5	3.7	159.7	-6.1	9.1
	132.8	-0.8	4.7	157.6	-4.3	11.9
	132.5	-0.8	4.6	158.6	-6.9	10.3
	132.2	-1.2	4.7	156.9	-7.1	11.4
	⋮	⋮	⋮	⋮	⋮	⋮
$\bar{\kappa}_I \ \bar{\kappa}_J \ \bar{\kappa}_K$	132.6	-1.3	4.5	159.2	-6.4	10.6
$\bar{\kappa}/D$	$\begin{pmatrix} 131.3 & 4.5 \\ \bullet & 133.8 \end{pmatrix}$			$\begin{pmatrix} 152.8 & 10.6 \\ \bullet & 165.5 \end{pmatrix}$		
<b>S/D</b> <sup>2</sup>	$\begin{pmatrix} 0.097 & -0.073 & 0.053 \\ \bullet & 0.269 & -0.055 \\ \bullet & \bullet & 0.154 \end{pmatrix}$			$\begin{pmatrix} 0.987 & 0.211 & -0.069 \\ \bullet & 1.726 & 0.350 \\ \bullet & \bullet & 0.898 \end{pmatrix}$		

The means,  $\bar{\kappa}_I$ ,  $\bar{\kappa}_J$  and  $\bar{\kappa}_K$ , of the 25 sets of coefficients, are obtained simply as the arithmetic means of the coefficients. They are listed for the front and back surfaces in Table 3. Combining the coefficients according to Equation (4) of a previous paper<sup>2</sup> we obtain the mean surface curvature matrices  $\bar{\kappa}$  for the front and back surfaces of the cornea (see Table 3). The eigenstructure of  $\bar{\kappa}$  gives the principal meridians of the mean surface curvature and the curvatures along them (last row of Table 2); from these principal curvatures one obtains the corresponding radii of

curvature (last row of Table 1).

The variance-covariance matrices **S** based on the coordinate vector  $(\kappa_I \ \kappa_J \ \kappa_K)^T$  are also given in Table 3. Because the matrices are symmetric only the entries in the upper-triangular portions of the matrices need be shown.

Figure 1 is a stereo-pair plot representing the surface curvatures in surface curvature space. The dots in (b) and (c) correspond to the coordinates listed in Table 3. The estimated ellipsoidal surfaces of constant probability density that enclose 95% of the population are shown by means of their principal ellipses and principal diameters. Red represents the front surface of the cornea and green the back surface. The origin in (a) represents null surface curvature, that is, a flat surface. The two ellipsoids, small in (a) are re-drawn in (b) and (c) at a larger scale and shifted so that the centroids of the ellipsoids are at the origin.

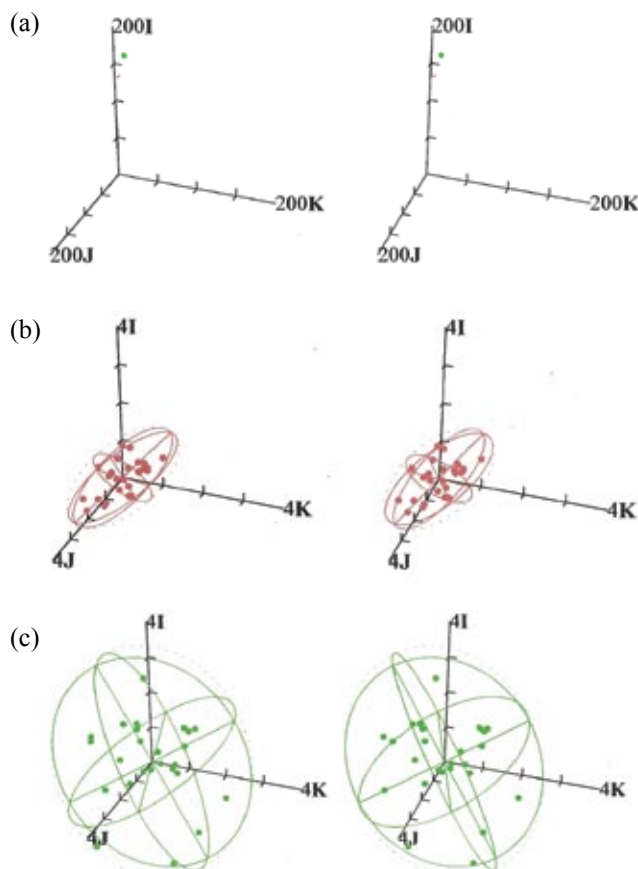


**Figure 1** Stereo-pair plots of ellipsoidal surfaces of constant probability density (enclosing 95% of the population) in surface curvature space of the surface curvatures of the anterior (red) and posterior (green) surfaces of the cornea. In (a) the origin represents null curvature (a flat surface). The ellipsoids reduce to a small red dot and a larger green dot just to the right of the vertical axis in this orientation. In (b) the ellipsoid for the anterior surface is repeated at a larger scale and with the mean curvature (given in Table 3) at the origin. (c) shows the same but for the posterior surface. The dots in (b) and (c) represent 25 surface curvatures calculated from individual measurements (the first five of which are listed in Table 3).



It is immediately evident from these results that the back surface of the cornea exhibits greater variation in surface curvature than the front surface. This is in marked contrast to what is observed<sup>1</sup> with surface powers.

**Surface curvatures referred to the corneal mid-surface**

The notion of global and local curvature of the cornea requires the front and back surfaces to be referred to a common location such as the mid-corneal surface. This is done for the anterior and posterior surfaces by means of Equations (15) and (16) of the previous paper<sup>2</sup>. The results are shown in Table 4 for the surface curvatures referred to the corneal mid-surface. Figure 2 shows the results graphically.

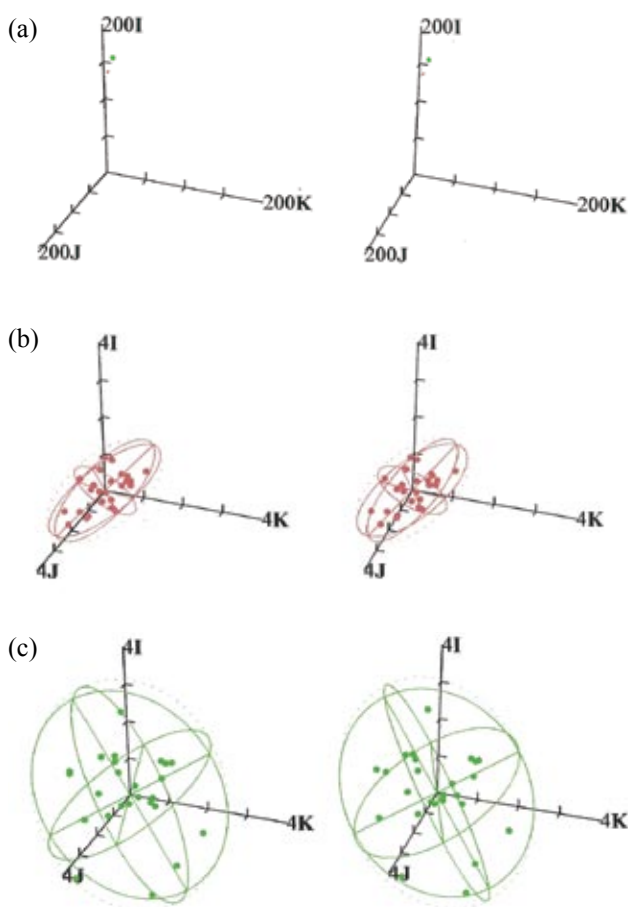


**Figure 2** As for Figure 1 except that the surface curvatures are referred to the corneal mid-surface. The red ellipsoid (anterior surface) is slightly enlarged in (b) and slightly further from the origin in (a). The green ellipsoid (posterior surface) is slightly reduced in size in (c) and slightly closer to the origin in (a). The red and green ellipsoids in (a) are closer together than in Figure 1(a).

**Table 4** The same as Table 3 except that the curvatures are referred to the mid-corneal surface.

			Anterior surface			Posterior surface		
			$\kappa_I/D$	$\kappa_J/D$	$\kappa_K/D$	$\kappa_I/D$	$\kappa_J/D$	$\kappa_K/D$
			136.9	-1.8	4.5	155.7	-6.8	9.4
			136.4	-1.6	4.0	154.5	-5.7	8.5
			136.6	-0.9	5.0	152.6	-4.1	11.2
			136.3	-0.9	4.8	153.5	-6.5	9.6
			136.0	-1.2	4.9	151.9	-6.7	10.7
			⋮	⋮	⋮	⋮	⋮	⋮
$\bar{\kappa}_I$	$\bar{\kappa}_J$	$\bar{\kappa}_K$	136.3	-1.3	4.7	154.0	-6.0	9.9
			$\begin{pmatrix} 135.0 & 4.7 \\ \bullet & 137.7 \end{pmatrix}$			$\begin{pmatrix} 148.1 & 9.9 \\ \bullet & 160.0 \end{pmatrix}$		
			$\begin{pmatrix} 0.105 & -0.079 & 0.054 \\ \bullet & 0.301 & -0.061 \\ \bullet & \bullet & 0.172 \end{pmatrix}$			$\begin{pmatrix} 0.881 & 0.184 & -0.079 \\ \bullet & 1.518 & 0.303 \\ \bullet & \bullet & 0.786 \end{pmatrix}$		

Figure 2(a) shows that the red ellipsoid (shown as a tiny dot) has moved a little further from the origin in comparison with its position in Figure 1(a) while the green one has moved a little closer to the origin. Referring the surface curvatures to the corneal mid-surface has caused the two ellipsoids to move towards each other. Purely global variation in curvature about the mid-surface would mean that the two ellipsoids would coincide. Their distance apart reflects the amount of local variation in curvature.

Relative to the ellipsoid in Figure 1(b) the ellipsoid in Figure 2(b) is slightly enlarged. On the other hand relative to the ellipsoid in Figure 1(c) the ellipsoid in Figure 2(c) is slightly smaller. Referring the curvature to the mid-surface has no effect on the shape of the ellipsoids.

**Global and local curvatures of the cornea**

The global curvature of the cornea is calculated by means of Equation (17) of the previous paper<sup>2</sup>. It is merely the semi-sum (the arithmetic mean) of the curvatures of the anterior and posterior surfaces referred to the mid-surface. The local contribution to corneal curvature is given by Equation (18) of that paper (it is a semi-difference of the two curvatures referred to the mid-surface); it is in terms of the back surface relative to the front surface. The results are summarized in Table 5 and Figure 3. The mean global and local contributions to curvature are given as matrices in Table 5. Expressed in principal meridional form the mean global curvature is 137.0 D along 148° and 153.4 D and the mean local contribution is 5.4 D along 156° and 12.3 D.



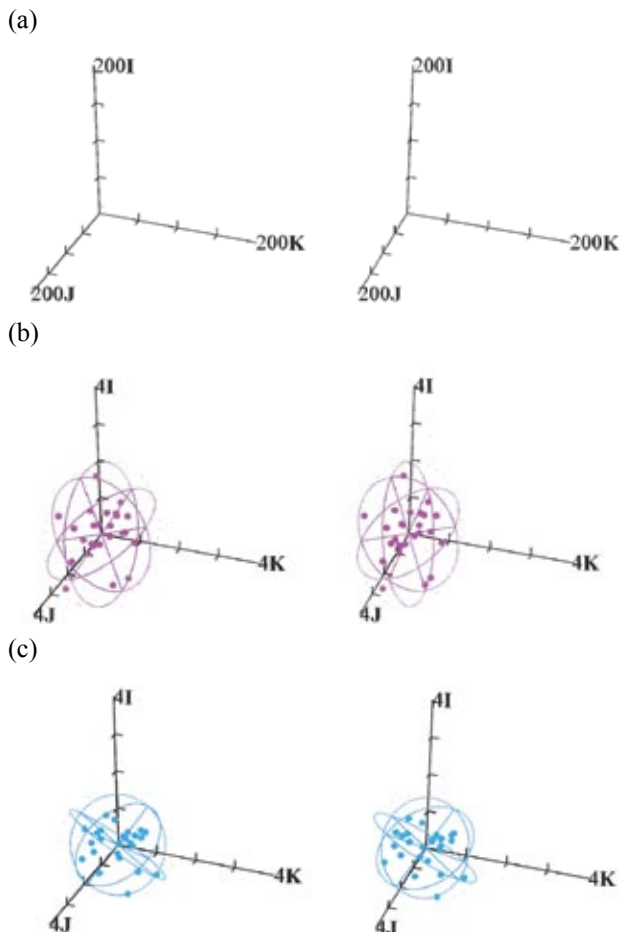


**Figure 3** Stereo-pair plots of ellipsoidal surfaces of constant probability density (enclosing 95% of the population) in surface curvature space of the global (magenta) and local (cyan) curvatures of the cornea. Both are shown in (a) with null curvature at the origin. The global contribution is shown in (b) and the local contribution in (c) with the centroids of the ellipsoids shifted to the origin. The local contribution (just noticeable in (a) close to the origin) is much less in magnitude than the global contribution (close to the surface curvature 150I D). The global surface curvature (b) exhibits greatest variation in a direction roughly parallel to axis J. The ellipsoid for the local contribution (c) is roughly spherical in the space.

**Table 5** Global and local contributions to curvature of the cornea.

	Global contributions			Local contributions		
	$\kappa_I / D$	$\kappa_J / D$	$\kappa_K / D$	$\kappa_I / D$	$\kappa_J / D$	$\kappa_K / D$
	146.3	-4.3	6.9	9.4	-2.5	2.4
	145.5	-3.7	6.2	9.1	-2.1	2.3
	144.6	-2.5	8.1	8.0	-1.6	3.1
	144.9	-3.7	7.2	8.6	-2.8	2.4
	143.9	-4.0	7.8	8.0	-2.7	2.9
	⋮	⋮	⋮	⋮	⋮	⋮
$\bar{\kappa}_I \quad \bar{\kappa}_J \quad \bar{\kappa}_K / D$	145.2	-3.6	7.3	8.9	-2.3	2.6
$\bar{\kappa} / D$	$\begin{pmatrix} 141.5 & 7.3 \\ \bullet & 148.8 \end{pmatrix}$			$\begin{pmatrix} 6.5 & 2.6 \\ \bullet & 11.2 \end{pmatrix}$		
$S/D^2$	$\begin{pmatrix} 0.286 & 0.012 & -0.034 \\ \bullet & 0.659 & 0.043 \\ \bullet & \bullet & 0.189 \end{pmatrix}$			$\begin{pmatrix} 0.207 & 0.042 & 0.022 \\ \bullet & 0.250 & 0.081 \\ \bullet & \bullet & 0.290 \end{pmatrix}$		

The global curvature of the cornea is represented by the magenta dot close to surface curvature 150I D in Figure 3(a). It lies halfway between the red and green dots in Figure 2(a). It represents an average of the curvatures of the anterior and posterior surfaces both referred to the corneal mid-surface. The local contribution to corneal curvature is much smaller in magnitude; the tiny cyan dot that represents it lies close to axis I and just above the origin in Figure 3(a).

The ellipsoid representing the local variation in curvature is not far from being spherical in the space as is evidenced by Figure 3(c) and the variance-covariance matrix in Table 5. This is in keeping with what one expects for small-scale effects.<sup>3</sup> On the other hand the ellipsoid representing variation in global curvature is definitely stretched in Figure 3(b) in a direction nearly parallel to axis J a fact also revealed by the large central entry (the variance of the ortho-antispherical coordinate  $\kappa_J$ ) in the variance covariance-matrix. This is indeed in keeping with larger-scale or global effects.<sup>3</sup> More particularly the principal meridians associated with the ortho-antispherical variation (horizontal and vertical) suggest that the dominant cause of the variation may well be the lids and the blinking action.

**Concluding remarks**

The very simple model described elsewhere has been applied here, with some apparent success, to a moderately keratoconic cornea. The model shows that global effects of corneal curvature are dominant with the ortho-antispherical component in particular the most important. This in turn suggests that an important contribution to variation in curvature may be the lids and blinking. There was no attempt in this study to control blinking. Clearly future work needs to examine blinking in particular and also the normal, non-keratoconic cornea.

**References**

1. Gillan WDH. Variation in surface power and thickness of a moderately keratoconic cornea. *S Afr Optom* 2008 **67** 4-10.
2. Harris WF. Global and local contributions to corneal surface curvature: a simple model. *S Afr Optom* 2008 **67** 11-16.
3. Harris WF. Meridional profiles of variance-covariance of symmetric dioptric power: classes of variation that are uniform across the meridians of the eye. *Optom Vis Sci* 1997 **74** 397-413.

